Supplementary Materials

# Temporal and Spatial Characteristics of Multidimensional Extreme Precipitation Indicators: A Case Study in the Loess Plateau, China

**Chaoxing Sun [1], Guohe Huang [2,*] and Yurui Fan [3]**

[1] Institute for Energy, Environment and Sustainability Research, UR-NCEPU, North China Electric Power University, Beijing 102206, China; chaoxingsun2015@hotmail.com
[2] Center for Energy, Environment and Ecology Research, UR-BNU, Beijing Normal University, Beijing 100875, China
[3] Department of Civil and Environmental Engineering, Brunel University, London, Uxbridge, Middlesex UB8 3PH, UK; yurui.fan@brunel.ac.uk
* Correspondence:huang@iseis.org; Tel: +130-6585-4095; Fax: +130-6337-3205

**Table S1.** Statistical test comparisons between GMM and the best fitted ones of five other distributions (Gamma, Pearson type III (P III), lognormal (LN), Log Pearson type III (LP III), generalized extreme value (GEV)) at Yulin Station.

| Indices | Marginal Distribution | K–S Test | | RMSE | AIC |
|---|---|---|---|---|---|
| | | $T$ | *p* value | | |
| D95 | GMM | 0.143 | 0.568 | 0.055 | −170.089 |
| | P III | 0.149 | 0.515 | 0.057 | −165.732 |
| P95 | GMM | 0.089 | 0.972 | 0.029 | −208.096 |
| | LN | 0.100 | 0.925 | 0.044 | −183.023 |
| R95 | GMM | 0.082 | 0.987 | 0.032 | −202.164 |
| | GEV | 0.098 | 0.931 | 0.034 | −196.206 |

KS test: the Kolomogorov–Smirnov test; $T$ : the value of the test statistic; *p*-Value: the significance level; RMSE: root mean square error; AIC: Akaike's information criteria.

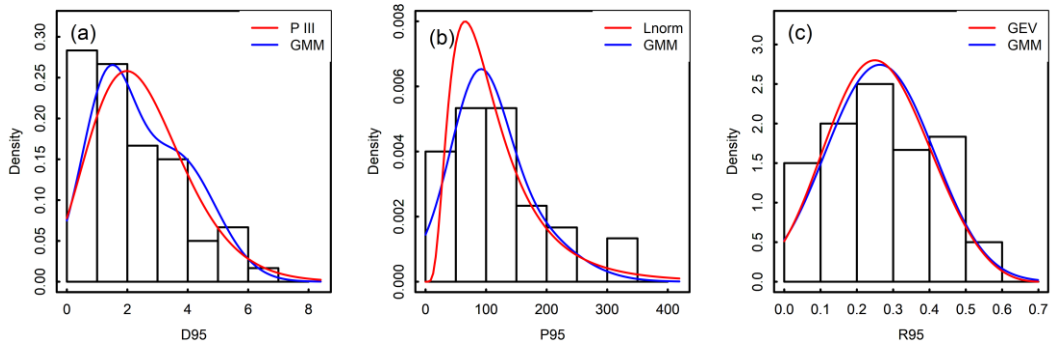


**Figure S1.** Comparisons between GMM and other probability density estimates with theoretical frequency at Yulin Station: (**a**) PDF for D95, (**b**) PDF for P95, (**c**) PDF for R95.

**Table S2.** Statistical test results for copulas at Yulin Station.

| Scheme | Copula | K–S Test | | RMSE | AIC |
|---|---|---|---|---|---|
| | | $T$ | *p* value | | |
| {D95, P95} | Gaussian | **0.022** | **0.615** | **0.0268** | **−215.108** |
| | t | 0.024 | 0.565 | 0.0281 | −211.342 |
| | Gumbel | 0.027 | 0.583 | 0.0287 | −209.534 |
| | Frank | 0.035 | 0.139 | 0.0298 | −208.795 |
| {D95, R95} | Gaussian | 0.024 | 0.470 | 0.0325 | −203.528 |
| | t | **0.024** | **0.697** | **0.0324** | **−203.671** |
| | Gumbel | 0.027 | 0.533 | 0.0330 | −202.592 |
| | Frank | 0.027 | 0.615 | 0.0327 | −203.219 |
| {P95, R95} | Gaussian | **0.028** | **0.790** | **0.0298** | **−208.887** |
| | t | 0.216 | 0.778 | 0.0310 | −206.908 |
| | Gumbel | 0.032 | 0.189 | 0.0315 | −205.409 |
| | Frank | 0.022 | 0.778 | 0.0311 | −206.172 |
| {D95, P95, R95} | Gaussian | 0.037 | 0.562 | 0.0231 | −225.227 |
| | t | **0.032** | **0.648** | **0.0214** | **−228.451** |
| | Gumbel | 0.052 | 0.172 | 0.0257 | −220.352 |
| | Frank | 0.048 | 0.418 | 0.0233 | −224.881 |

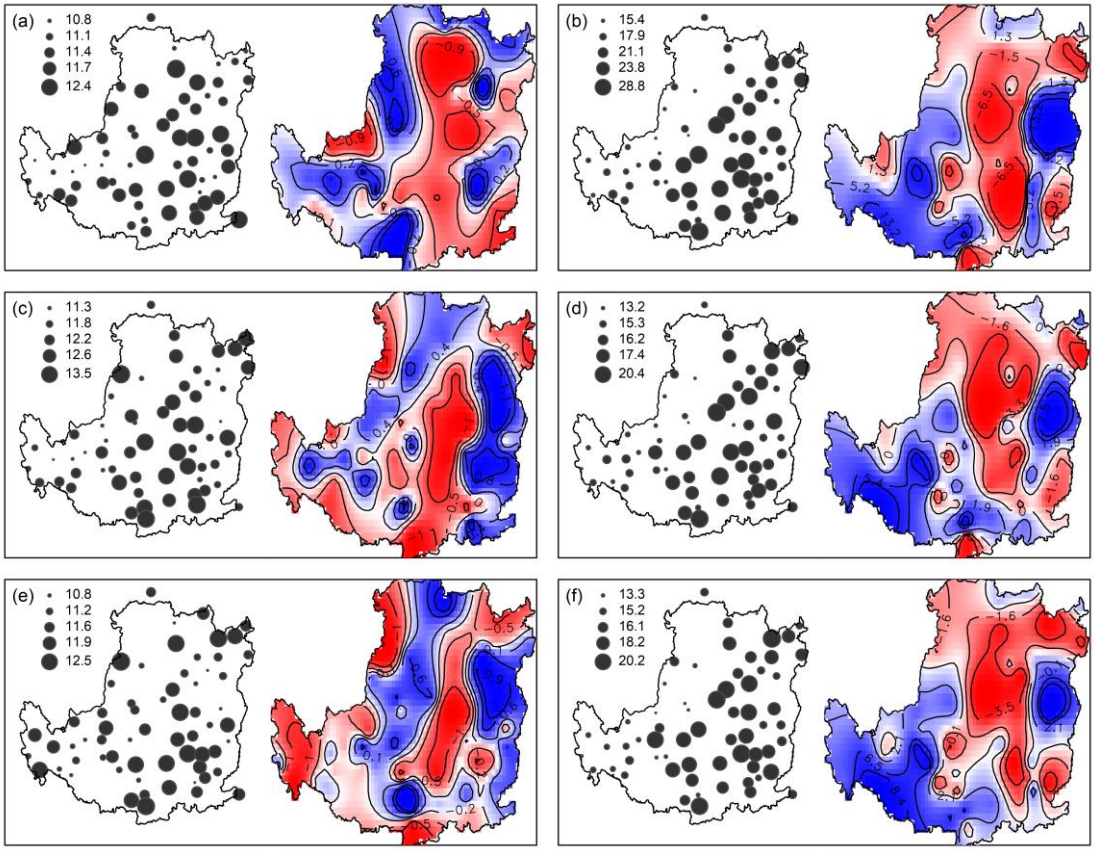


**Figure S2.** Joint return periods ($T_k$) at each station in 1959-1988 (left ones) and spatial changes in 1989-2018 (right ones) for six two-dimensional indicator combinations: (**a**) {D95, P95}, (**b**) {D95, I95}, (**c**) {D95, R95}, (**d**) {P95, I95}, (**e**) {P95, R95}, and (**f**) {I95, R95}.

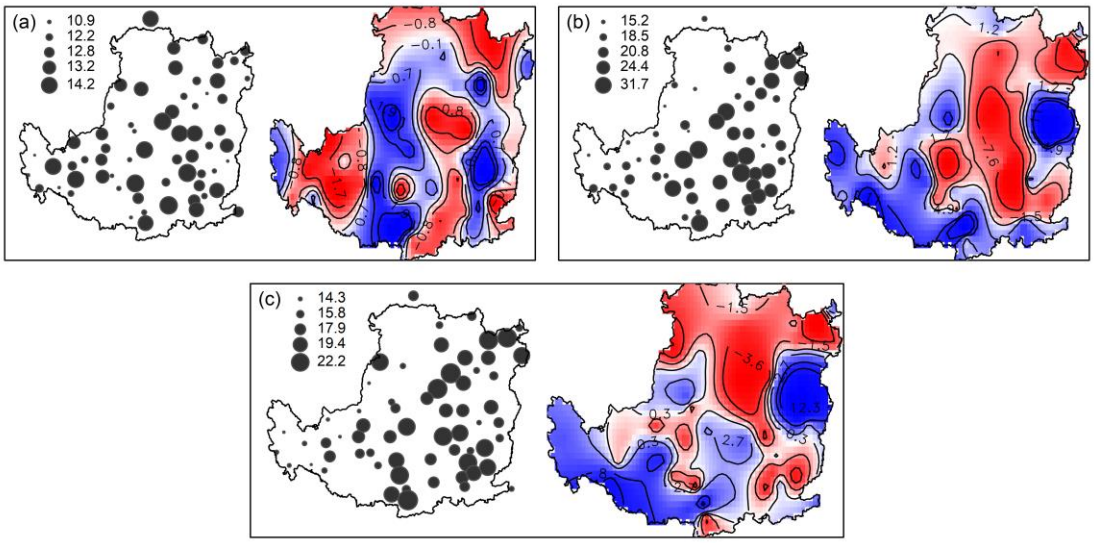


**Figure S3.** Joint return periods ($T_k$) at each station in 1959-1988 (left ones) and spatial changes in 1989-2018 (right ones) for three three-dimensional indicator combinations: (**a**) {D95, P95, R95}, (**b**) {D95, I95, R95}, and (**c**) {P95, I95, R95}.

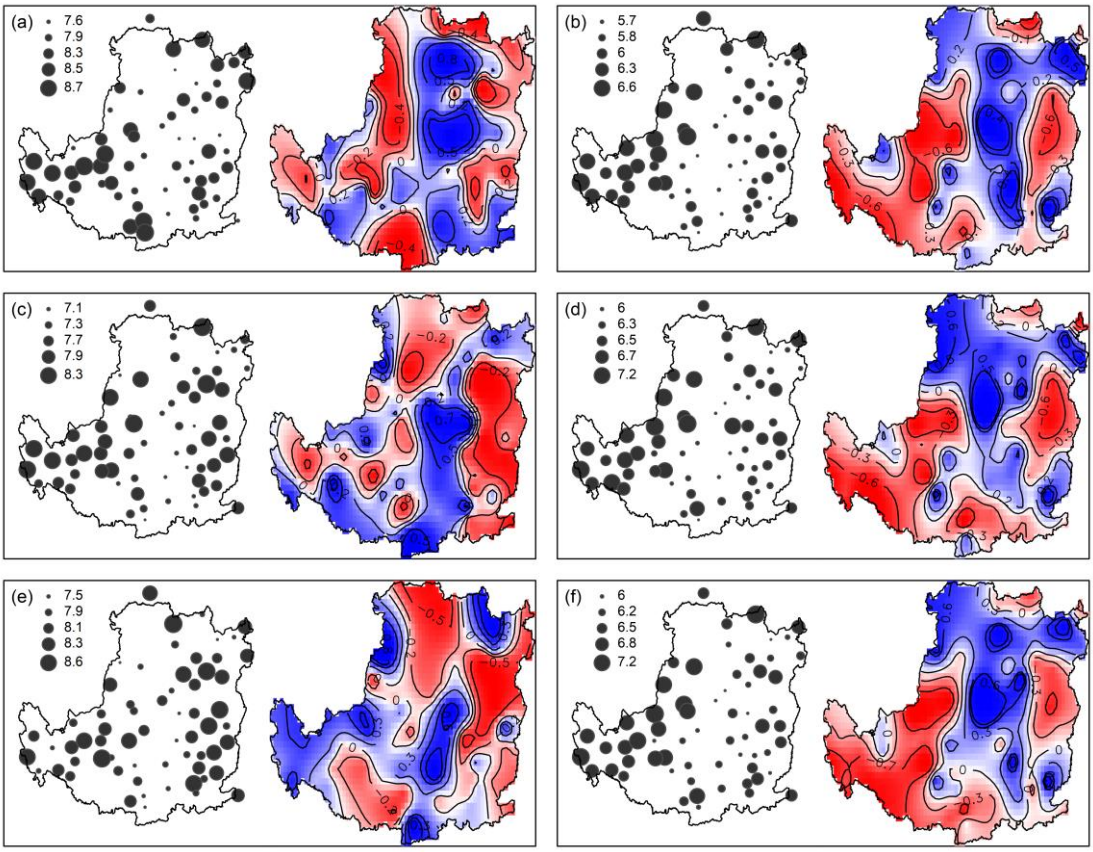


**Figure S4.** Joint return periods ($T_{or}$) at each station in 1959-1988 (left ones) and spatial changes in 1989-2018 (right ones) for six two-dimensional indicator combinations: (**a**) {D95, P95}, (**b**) {D95, I95}, (**c**) {D95, R95}, (**d**) {P95, I95}, (**e**) {P95, R95}, and (**f**) {I95, R95}.

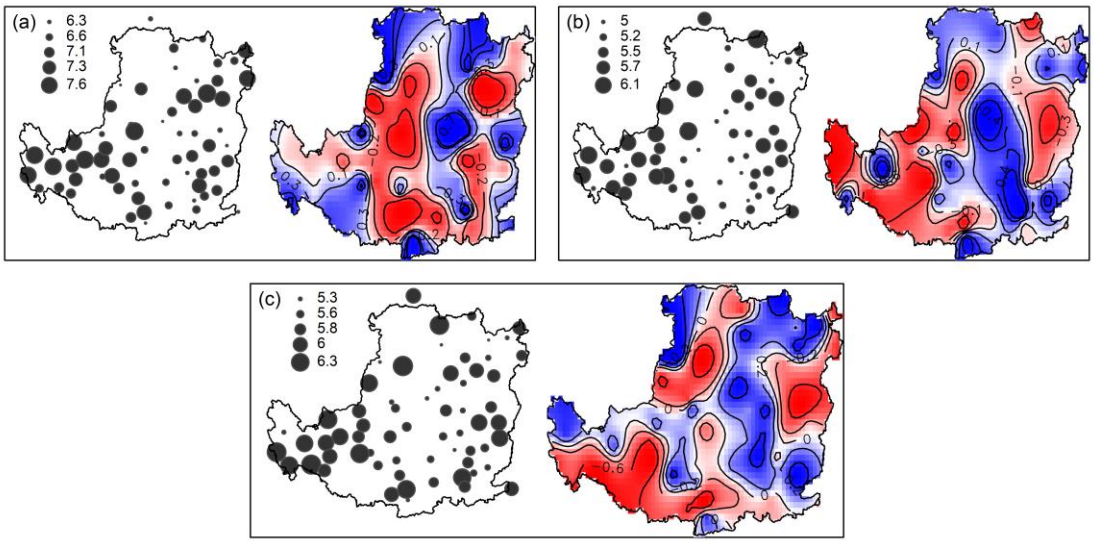


**Figure S5.** Joint return periods ($T_{or}$) at each station in 1959-1988 (left ones) and spatial changes in 1989-2018 (right ones) for three three-dimensional indicator combinations: (**a**) {D95, P95, R95}, (**b**) {D95, I95, R95}, and (**c**) {P95, I95, R95}.

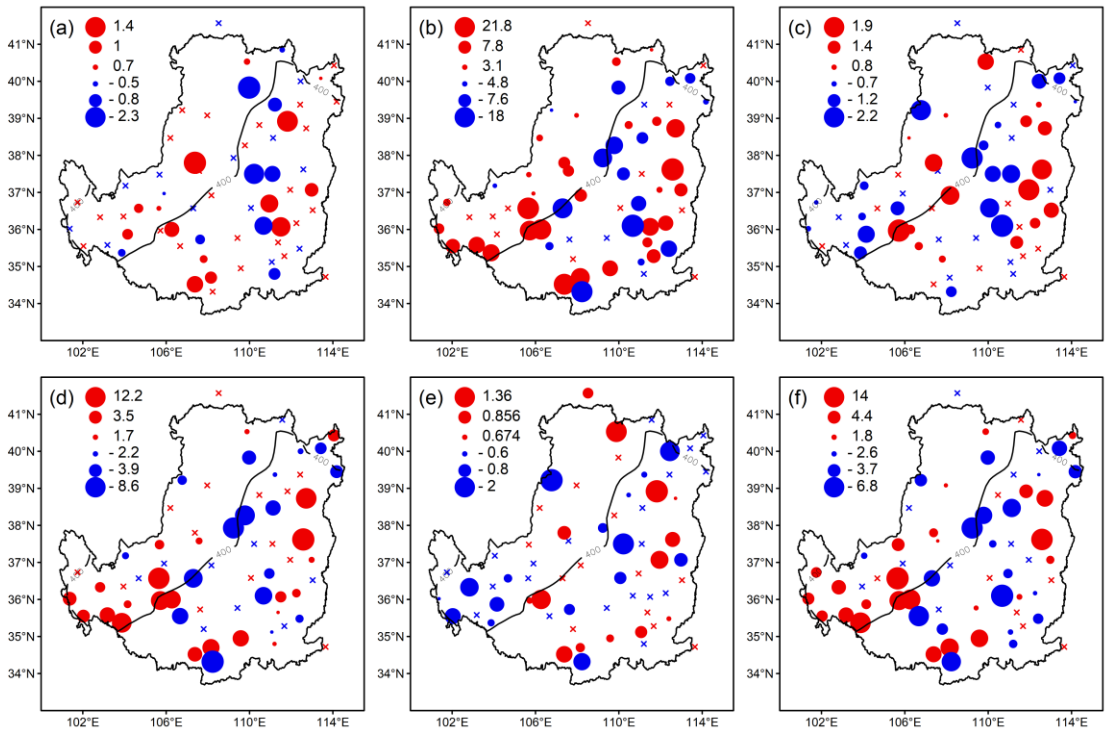


**Figure S6.** The significance and magnitude of the trends in joint return periods ($T_k$) over 30-year moving window series for six two-dimensional indicator combinations: (**a**) {D95, P95}, (**b**) {D95, I95}, (**c**) {D95, R95}, (**d**) {P95, I95}, (**e**) {P95, R95}, and (**f**) {I95, R95}.

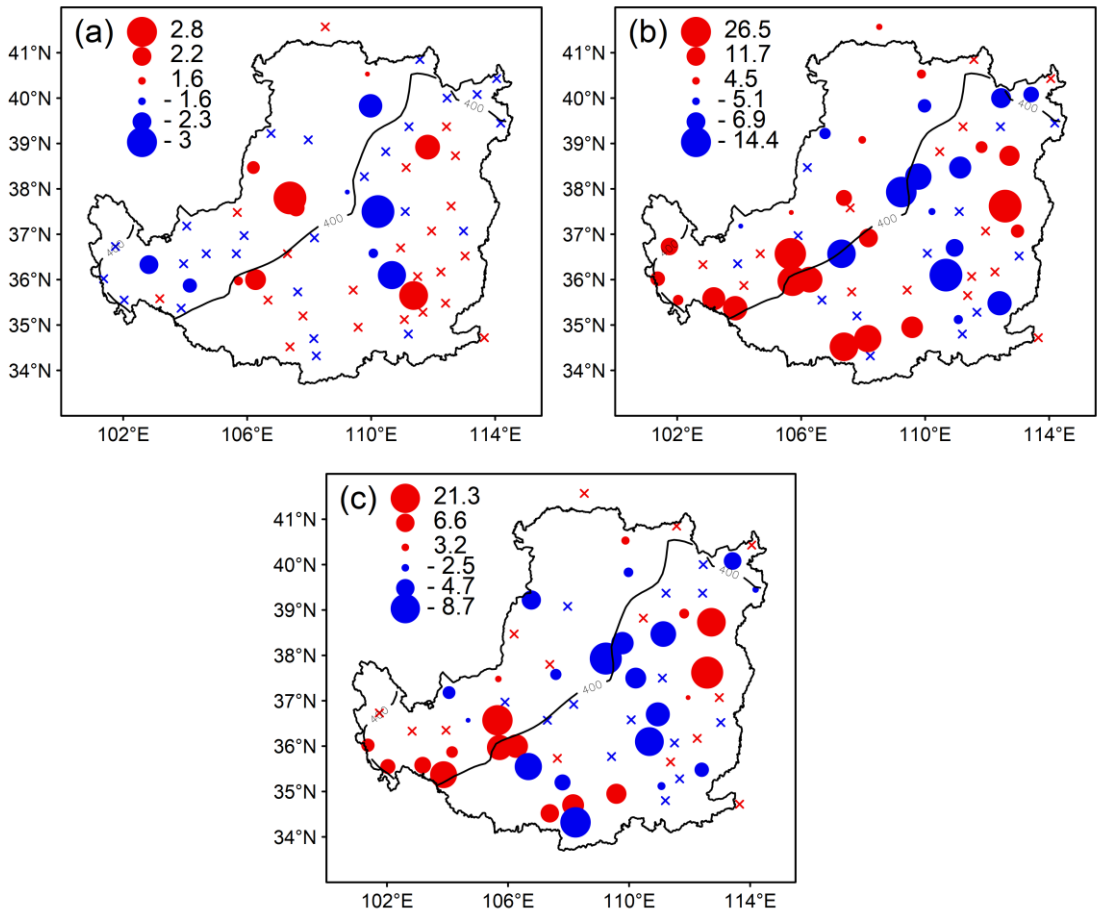


**Figure S7.** The significance and magnitude of the trends in joint return periods ($T_k$) over 30-year moving window series for three three-dimensional indicator combinations: (**a**) {D95, P95, R95}, (**b**) {D95, I95, R95}, and (**c**) {P95, I95, R95}.

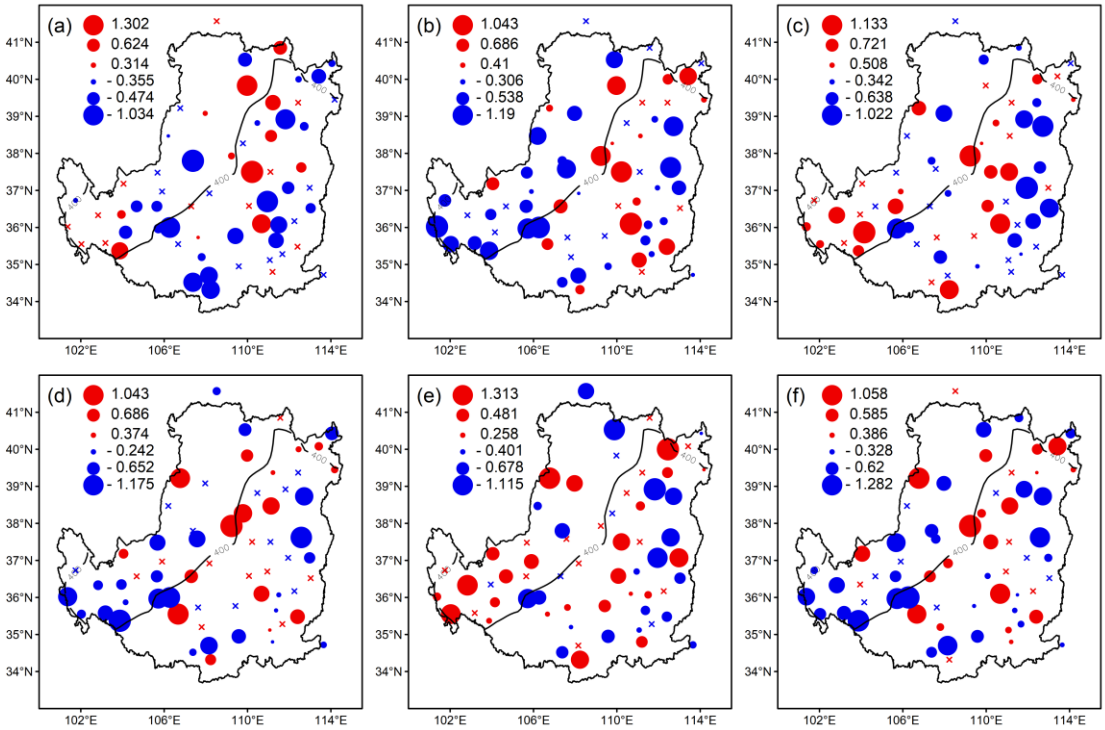


**Figure S8.** The significance and magnitude of the trends in joint return periods ($T_{or}$) over 30-year moving window series for six two-dimensional indicator combinations: (**a**) {D95, P95}, (**b**) {D95, I95}, (**c**) {D95, R95}, (**d**) {P95, I95}, (**e**) {P95, R95}, and (**f**) {I95, R95}.

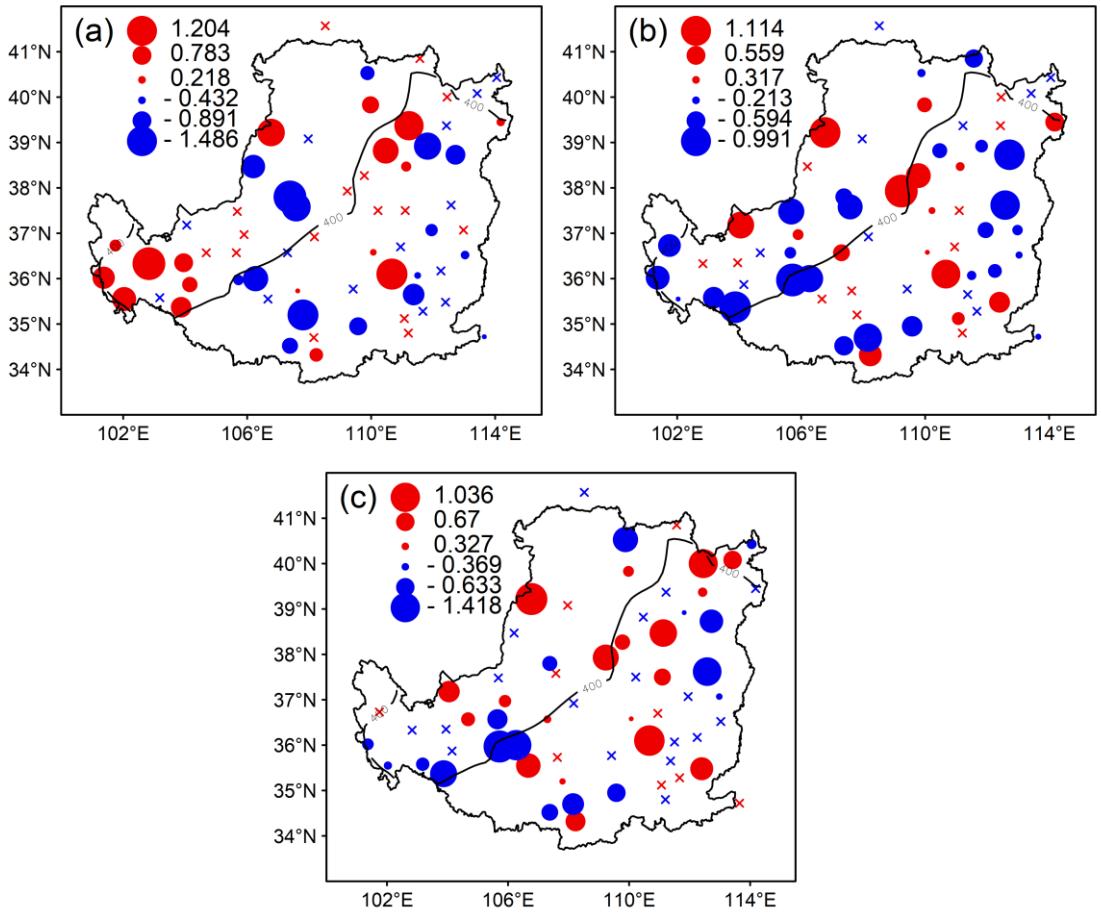


**Figure S9.** The significance and magnitude of the trends in joint return periods ($T_{or}$) over 30-year moving window series for three three-dimensional indicator combinations: (**a**) {D95, P95, R95}, (**b**) {D95, I95, R95}, and (**c**) {P95, I95, R95}.